ADVANCED ENERGY MATERIALS
www.advenergymat.de

Lithium Sulfide/Metal Nanocomposite as a High-Capacity Cathode Prelithiation Material

*Yongming Sun, Hyun-Wook Lee, Zhi Wei Seh, Guangyuan Zheng, Jie Sun, Yanbin Li, and Yi Cui**

Two approaches to increase specific energy and energy density of batteries include the exploration of new battery chemistries and the continuous improvement of the existing lithium-ion battery (LIB) chemistries.[1,2] The exploration of new high-capacity electrode materials, such as Si for anodes and S/Li_2S for cathodes, has recently become an important focus of materials research and will potentially revolutionize energy storage technologies.[3,4] At the same time, the improvement of the existing LIB systems could also offer more practical avenues and faster performance increment in the near future. Accompanied by the formation of a solid electrolyte interphase (SEI) layer on the anode surface during the initial battery charge process, some lithium from the cathode is consumed, which reduces appreciably the specific energy and energy density of current LIBs (5%–20% of a total battery capacity).[5–8] In the past few years, increased efforts have been devoted to exploring prelithiation strategies to compensate for the initial lithium loss of LIBs. Although electrochemical prelithiation approaches have been successfully demonstrated, an electrochemical cell needs to be built and disassembled, resulting in complex operations.[9,10] Sacrificial lithium salts can be used as prelithiation additives to electrolytes or electrodes. However, as Armand and co-workers mentioned, undesired gas, such as N_2, CO, or CO_2, was produced upon the release of lithium.[11] Specifically designed prelithiation additives to electrodes can deliver high "donor" lithium-ion specific capacities to offset the initial lithium loss and hence improve the electrochemical performance of current LIBs. To date, anode prelithiation materials, including stabilized lithium metal powders[12–15] and lithium silicide particles,[16,17] have been investigated due to their high specific capacities. However, their high chemical reactivity and instability under ambient and battery fabrication conditions remain as challenges. Cathode prelithiation materials have relatively high open circuit voltage (OCV) and chemical stability, offering another attractive route. However, little success has been shown on the cathode prelithiation materials, probably due to their limited specific capacity.[18,19] Very recently, we have proposed that conversion reaction materials can be attractive high capacity prelithiation materials for cathodes and demonstrated using Li_2O/metal and LiF/metal nanocomposites.[20,21] For example, a high "donor" lithium-ion specific capacity of 609 mAh g^{-1} has been achieved for a stable nanoscaled mixture of Li_2O and Co in the cutoff potential range of current cathodes.[20]

Herein, we would like to explore the potential of Li_2S and metal nanocomposites for cathode prelithiation. We believe that having a new set of lithium compounds beyond Li_2O for cathode prelithiation is important. Li_2S possesses a high theoretical specific capacity of 1166 mAh g^{-1} and can be paired with lithium free anodes (e.g., graphite, Sn, and Si). It has been widely investigated as one of the best cathode candidates for the next-generation rechargeable lithium batteries and significant achievements have been demonstrated.[22–26] Here we propose that Li_2S can be used as a high-capacity cathode prelithiation material for the existing LIBs. To this end, four significant challenges need to be overcome: (1) The compatibility of electrolytes. Previous investigations on pristine Li_2S and S particles for cathodes were usually carried out in ether-based electrolytes instead of the widely used carbonate-based electrolytes in commercial LIBs.[4,22,27,28] Because carbonate-based solvents chemically react with the intermediate polysulfides, such solvents are inappropriate for S and Li_2S cathodes.[29] (2) The compatibility of working potential. The widely used cathode materials usually have a cutoff charge potential higher than 4.2 V versus Li^+/Li (e.g., 4.3 V for $LiCoO_2$, $LiNi_xCo_yMn_zO_2$, and $LiMnO_4$, and 4.2 V for $LiFePO_4$) and a cutoff discharge potential higher than 2.5 V (e.g., 2.5–3 V) in the carbonate-based electrolytes. To maximize the "donor" lithium-ion capacity, relative low delithiation (e.g., <4.2 V) and lithiation potentials (e.g., <2.5 V) are desirable for a cathode prelithiation material, so that all the stored lithium can be irreversible extracted during the first charge/discharge cycle. (3) The diffusion of the intermediate polysulfides and low conductivity of Li_2S. Due to the loss of polysulfide active material into the electrolyte, it is challenging to maximize the lithium-ion capacity. Additionally, it is hard to extract lithium from Li_2S due to its insulating nature. (4) The instability under ambient and battery fabrication conditions. Li_2S is highly reactive with moisture in air. Such property makes it incompatible with ambient and industrial battery fabrication conditions. Despite the great knowledge obtained from the previous work on Li_2S-based cathode material, the solutions to this issue remain to be developed. Therefore, it is highly desirable to solve these inherent problems of Li_2S via a rational structure and component design to pave the path for its application as

Dr. Y. M. Sun, Dr. H.-W. Lee, Dr. Z. W. Seh,
Dr. G. Y. Zheng, Dr. J. Sun, Y. B. Li, Prof. Y. Cui
Department of Materials Science and Engineering
Stanford University
Stanford, CA 94305, USA
E-mail: yicui@stanford.edu
Prof. Y. Cui
Stanford Institute for Materials and Energy Sciences
SLAC National Accelerator Laboratory
Menlo Park, CA 94025, USA

DOI: 10.1002/aenm.201600154

Table 1. Comparison between Li_2S and Li_2S/metal (e.g., Li_2S/Co) composite.

	Reaction mechanism	Capacity [mAh g^{-1}]	Delithiation/lithiation potential (first)	Compatibility with carbonate electrolytes	Conductivity	Stability
Li_2S	$Li_2S \rightarrow 2Li^+ + S + 2e^-$	1166	<4.2 V/ <2.5 V	No		
Li_2S/Co	$Co + 2Li_2S \rightarrow CoS_2 + 4Li^+ + 4e^-$	711	<3 V/<2 V	Yes	Increased	Increased

a high-capacity cathode prelithiation material for the existing LIBs.

In this work, we propose that a novel class of Li_2S/metal nanocomposites made by thorough mixing of ultrafine Li_2S and metal particles can be used for high-capacity prelithiation of cathodes. Such design has multiple advantages to address the challenges that pristine Li_2S faces (**Table 1**): (1) After the introduction of metal to Li_2S, the lithium-extraction mechanism changes from a decomposition reaction ($Li_2S \rightarrow 2Li^+ + S + 2e^-$) to a conversion reaction ($xM + yLi_2S \rightarrow M_xS_y + 2yLi^+ + 2ye^-$). As shown by previous studies, such a conversion reaction works well in a carbonate-based electrolyte.[30–32] Therefore, the issue of incompatibility of electrolytes for Li_2S and existing cathode materials can be solved. (2) The electrochemical lithiation and delithiation of conversion sulfides take place below 2 and 3 V, respectively.[30–33] The low delithiation potential of Li_2S and metal composites leads to the full extraction of lithium from the additive below the cutoff charge potential of existing cathodes upon charging, while the low lithiation potential of metal sulfides makes sure that the lithium does not transform back to the initial state above the cutoff discharge potential of current cathodes. In other words, due to the potential limit, the conversion reaction of Li_2S/metal composites is one-way only for extracting lithium. Thus, as a cathode prelithiation additive, the "donor" lithium-ion capacity of the Li_2S/metal composites can be maximized. (3) The metal in the composites and the as-formed metal sulfide during the conversion reaction can immobile the polysulfide intermediates and prevent their irreversible reaction with the carbonate electrolytes.[34,35] Meanwhile, the metal sulfide can also act as a redox mediator to enhance the polysulfide redox reactions.[35] Therefore, there is no polysulfide dissolution problem for Li_2S/metal composite prelithiation materials. (4) The as-designed Li_2S/metal nanocomposites may have better ambient stability than that of pristine Li_2S particles, since the dense metal particles on the surface of the composite particles might help to suppress the penetration of moisture from air into the whole secondary particles. Meanwhile, similar to the previously reported Li_2O/metal and LiF/metal nanocomposites,[20,21] the metal nanoparticles in the Li_2S matrix can help to enhance the conductivity. Note that although the introduction of metal leads to the decrease of the overall theoretical specific capacity (e.g., 711 mAh g^{-1} for the Li_2S/Co composite), the real capacity would be increased due to the enhanced conductivity and stability.

Only with thorough mixing of nanoscale metal and lithium compound (e.g., <10 nm), can Li ions be effectively extracted via a conversion reaction.[20] Although the electrochemically formed nanocomposites of lithium compound (e.g., Li_2O, Li_2S, and LiF) and metal meet such a requirement for lithium extraction,[36,37] an easily scalable chemical synthesis route for lithium compound/metal composites is more desirable. Chemical conversion is an important route to synthesize nanocrystals.[38] Recently, the chemical reaction of sulfides and lithium has been monitored using in situ transmission electron microscopy (TEM) techniques.[39,40] The chemical conversion of sulfides (e.g., CoS_2, Co_3S_4, and FeS_2) to uniform Li_2S and metal nanocrystal composites (e.g., Li_2S/Co and Li_2S/Fe) has been directly observed. The features of intimate mixing and ultrafine particle size of the as-formed Li_2S/metal composites are ideal for extracting lithium upon the electrochemical charge process. With this knowledge in mind and the previous experiences on the synthesis of Li_2O/metal nanocomposites,[20] we have successfully fabricated Li_2S/metal (Li_2S/Co and Li_2S/Fe) nanocomposites via a chemical conversion reaction using metal sulfide (CoS_2 and FeS_2) particles and lithium metal as the starting materials. The lithium in the composites can be electrochemically extracted during battery charge via an inverse electrochemical conversion reaction in the first cycle (**Figure 1**). The as-synthesized nanocomposites have good compatibility with the current cathodes and exhibit high "donor" lithium-ion capacities (e.g., 670 mAh g^{-1} for a Li_2S/Co nanocomposite).

As a representative example, a Li_2S/Co nanocomposite was first prepared and characterized. During the synthesis, a lithium metal foil was first melted at 185 °C in argon atmosphere. Then CoS_2 powder was added according to the stoichiometric ratio based on the reaction equation ($CoS_2 + 4Li \rightarrow Co + 2Li_2S$). The Li_2S/Co nanocomposite was finally achieved after mechanical stirring at 185 °C for 20 min and at 220 °C for 2 h. The chemical transformation from the initial CoS_2 to Co/Li_2S product was characterized systematically. X-ray diffraction (XRD) results show that the initial sharp diffraction peaks of CoS_2 (JCPDS No. 41-1471) are replaced with broad diffraction peaks of Co (JCPDS No. 15-0806) and Li_2S (JCPDS No. 23-0369) after the reaction (**Figure 2**a,b), suggesting the chemical

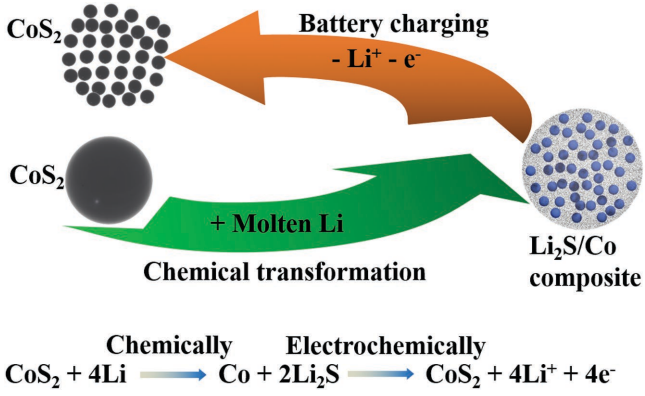

Figure 1. Schematic of the chemical synthesis of Li_2S/metal (e.g., Li_2S/Co) composite and the electrochemical extraction of lithium during the battery charge process.

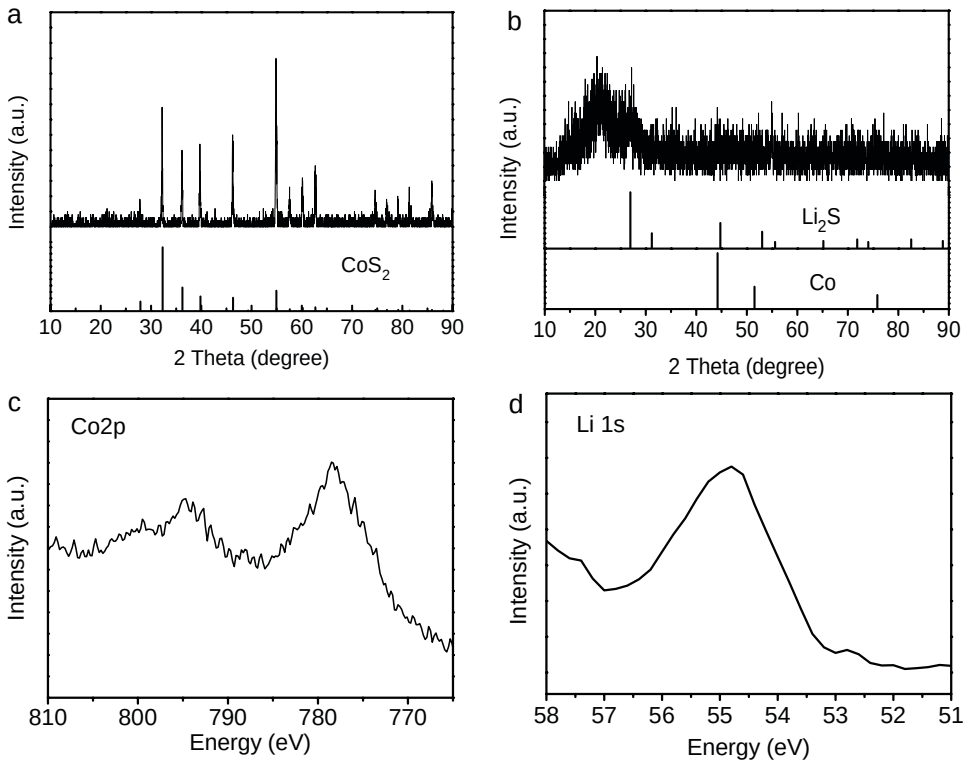

Figure 2. XRD patterns of a) the starting CoS_2 and b) Li_2S/Co product. High-resolution XPS spectra of c) Co 2p3 and d) Li 1s for the Li_2S/Co nanocomposite. The XRD peak at 21° arises from the Kapton tape, which is used to protect Li_2S from moisture in the air.

transformation from large CoS_2 particles to small Li_2S and Co nanodomains. Compared with the starting CoS_2, no obvious overall morphology change is observed for the as-synthesized Li_2S/Co nanocomposite under scanning electron microscopy (Figure S1, Supporting Information). Therefore, the chemical conversion does not destroy the original morphology, although it converts the chemical compositions and microstructure of the materials. The feature of a large secondary particle size in micrometer order remains after the chemical transformation reaction, which can help to stabilize the Li_2S-based composites in ambient air due to the low exposed surface area. High-resolution Co 2p and Li 1s X-ray photoelectron spectroscopy (XPS) was also performed to investigate the surface electronic state of the Li_2S/Co nanocomposite. Two peaks at 793.7 and 778.5 eV are observed in the high-resolution Co 2p spectrum, which can be assigned to the Co 2p 1/2 and Co 2p 3/2 spin-orbit peaks of Co (Figure 2c).[41] The high-resolution Li 1s XPS spectrum can be fitted with a single peak with a binding energy of 54.8 eV, corresponding to Li in the Li—S bond (Figure 2d).[23,42] Thus, the existence of Li_2S/Co composite is further confirmed.

TEM was also carried out to investigate the microstructure of the Li_2S/Co nanocomposite (**Figure 3**). After the chemical transformation reaction, the initial CoS_2 particles with a size ranging from 300 to 600 nm transformed to a uniform composite with much smaller particles (Figure S2, Supporting Information, and Figure 3a). The light/dark contrast in the STEM image is clearly observed (Figure 3b). The light region can be assigned to the Li_2S matrix, while the dark area suggests the presence of Co nanoparticles with higher mass density. The formed Li_2S and Co nanodomains are densely packed without cracks/pores. Therefore, the formation of a nanocomposite with Co nanoparticles embedded in a Li_2S matrix is verified. A high-magnification TEM image further confirms the finely dispersed Co nanoparticles in the Li_2S matrix (Figure 3c). High-resolution TEM (HRTEM) image shows that both the Co and Li_2S domains are crystalline with particle sizes of ≈5 nm (Figure 3d), in accordance with the XRD result (Figure 2b). Compared to the free CoS_2, the introduction of metallic Co nanoparticles in the composite enhances the electronic conductivity. The intimate mixing of Li_2S and Co nanocrystal domains can maximize the extracted lithium-ion capacity via an inverse conversion reaction upon battery charging. The dense Co domains in the structure might help to insulate Li_2S from the ambient air and thus improve the ambient stability of the Li_2S/Co composite.

To investigate the "donor" lithium-ion specific capacity of the as-made Li_2S/Co nanocomposites, galvanostatic discharge/charge measurement of the pristine Li_2S/Co electrode was carried out in the voltage range of 4.0–2.5 V versus Li^+/Li at the current density of 50 mA g^{-1}. To match their application in current LIBs, a carbonate-based electrolyte was used instead of ether-based electrolytes usually used for Li_2S-based electrodes. A reasonably high OCV is observed (1.5 V), compatible with the existing cathodes. The lithium extraction from the Li_2S/Co nanocomposite occurs upon charging in the potential range of 3.2–4.0 V, which is lower than the working potential for Li_2O and LiF based nanocomposites.[20,21] For conversion reaction based cathode additives, large amounts of charge transfer during the electrochemical lithium extraction process can lead

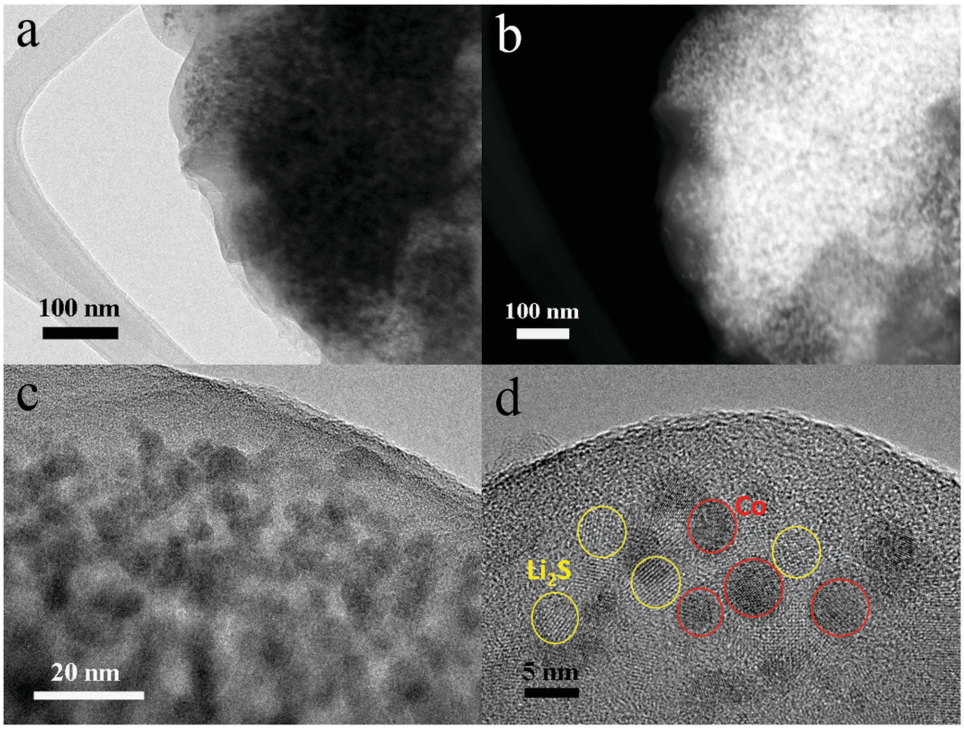

Figure 3. a) Low-magnification TEM, b) STEM, c) high-magnification TEM, and d) HRTEM images of the Li_2S/Co nanocomposite, showing the intimate mixing of Li_2S and Co nanocrystal domains with particle sizes of ≈5 nm.

to a high lithium-ion specific capacity. In principle, four lithium ions can be extracted for a Li_2S/Co (molar ratio of 2/1) nanocomposite to form a CoS_2 product ($Co + 2Li_2S \rightarrow CoS_2 + 4Li^+ + 4e^-$) during the charge process, giving rise to a high theoretical specific capacity of 711 mAh g^{-1}. As expected, the as-synthesized Li_2S/Co nanocomposites deliver a charge specific capacity of 683 mAh g^{-1} (**Figure 4**a), which is higher than that of the previously reported Li_2O/Co and LiF/Co nanocomposites.[20,21] Therefore, it can be expected that, when used as a prelithiation additive for the existing cathodes, almost the full lithium in the nanocomposite can be extracted upon charging below the cutoff charge potential of existing cathodes. During the discharge process, due to the potential limit, the additive does not transform back to its initial lithiated state above the cutoff discharge potential of the current cathodes. The specific discharge capacity of the Li_2S/Co nanocomposite is only 13 mAh g^{-1} above the cutoff potential of 2.5 V (Figure 4a). Therefore, the Li_2S/Co nanocomposite has a noticeable high "donor" lithium-ion specific capacity of 670 mAh g^{-1} in the first cycle, which is more than three times that of the existing cathodes. Cyclic voltammetry of a Li_2S/Co electrode was performed at a scanning rate of 0.2 mV s^{-1} (Figure S3a, Supporting Information). The Li_2S/Co electrode shows a broad oxidation peak in the potential range of 2–3.5 V in the first cycle, which disappears in the second cycle, indicating that the reaction of Li_2S/metal composites is one-way only for extracting lithium, not reversible during battery charging and discharging. To confirm the inverse conversion reaction mechanism of the as-achieved electrode upon charging, we performed XPS investigations on the Li_2S/Co electrode at the full charge state. The high-resolution Co 2p spectrum shows two peaks at 793.8 and 778.8 eV, which can be ascribed to Co^{2+} species of CoS_2 (Figure S4a, Supporting Information).[42,43] The breadth of the S 2p peak suggests the existence of multiple chemical states. The dominant structure shows a pair of S 2p1/2 and S 2p3/2 doublets at 162.4 and 163.9 eV, which are attributed to the CoS_2 phase (Figure S4b, Supporting Information).[43–45] An additional peak located at 169.1 eV is also detected, corresponding to sulfur oxide species.[43] Therefore, CoS_2 is confirmed as the charge product and the following conversion reaction mechanism is verified: $Co + 2Li_2S \rightarrow CoS_2 + 4Li$. Meanwhile, the high-resolution Co2p spectrum shows that the dominant Co2p3/2 peak of the Li_2S/Co composite electrode after the first charge/discharge cycle is centered at 778.8 eV and the Co2p1/2 features at 794.0 eV, corresponding to the cobalt oxidation state in CoS_2 (Figure S5, Supporting Information),[42,43] indicating that the involved conversion reaction is one-way and not reversible in the working potential of cathodes. The amount of prelithiation additives needed in a battery depends on the amount of lithium to form the SEI and the "donor" lithium-ion specific capacity of the additives. The high "donor" lithium-ion capacity suggests that the initial lithium loss in existing lithium-ion batteries can be offset with small amount of such an additive. Moreover, the reasonably high OCV and high "donor" charge specific capacity are important factors for the application of the Li_2S/Co composite in existing LIBs.

The stability and compatibility with current battery fabrication conditions is also vital for the practical application of prelithiation materials. Li_2S is very sensitive to moisture in comparison to LiF. Therefore, it is desirable but challenging that the hybrid cathodes with the Li_2S/Co additive can be fabricated in ambient air. To study compatibility with existing industrial battery

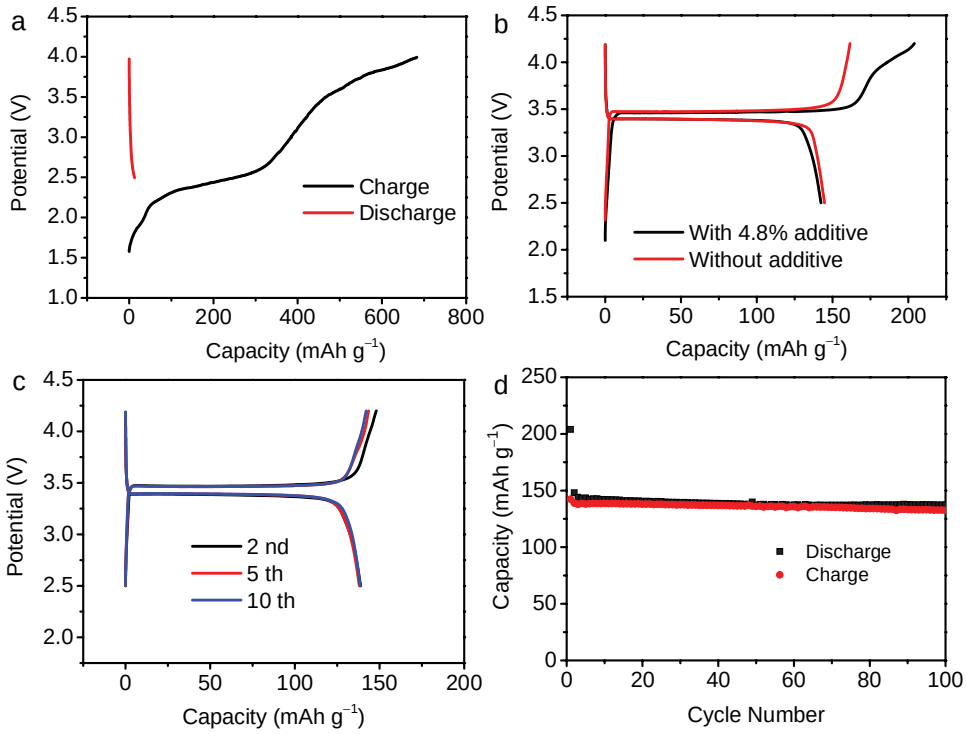

Figure 4. a) Voltage profiles of the first charge/discharge for pristine Li_2S/Co electrode at the current density of 50 mA g^{-1} with the potential range of 4.0–2.5 V versus Li^+/Li. b) The comparison of the first-cycle charge and discharge curves of $LiFePO_4$ electrode with and without the Li_2S/Co additive at 0.1 C in the potential range of 4.2–2.5 V versus Li^+/Li. c) Voltage profiles and d) cyclibility of a $LiFePO_4$ electrode with 4.8% Li_2S/Co additive.

processing conditions and the lithium compensation effect of the Li_2S/Co additive, the Li_2S/Co nanocomposite was added as a prelithiation reagent to a commercial $LiFePO_4$ material for electrode fabrication. The slurry coating and baking were all carried out in ambient atmosphere using a regular solvent (*N*-methyl-2-pyrrolidone) and a binder (polyvinylidene fluoride). The electrochemical performances of the $LiFePO_4$ electrode with the Li_2S/Co additive were performed in half cells with lithium metal as the counter/reference electrodes. During the first charge process, the $LiFePO_4$ with 4.8% Li_2S/Co additive shows obvious potential slops and increased charge specific capacity in comparison to the pristine $LiFePO_4$ electrode (Figure 4b), indicating the additive does not lose the lithium-ion activity during the electrode fabrication process. The success extraction of lithium from the additive in the hybrid electrode fabricated in ambient air indicates that the as-prepared nanostructure of Li_2S/Co nanocomposite improves the moisture stability of Li_2S. Notably, the $LiFePO_4$ electrode with 4.8% Li_2S/Co additive delivers a high initial charge specific capacity of 204 mAh g^{-1} at 0.1 C, 42 mAh g^{-1} higher than that of the pristine $LiFePO_4$ electrode. The lithium compensation efficiency is determined by the "donor" lithium-ion capacity of the additives. If the additive can deliver a higher "donor" lithium-ion capacity, less additive will be needed in a full cell to compensate for the initial lithium loss, leading to a higher overall capacity and energy density of full cells. Here, the high initial charge capacity of the as-prepared hybrid cathode indicates good prelithiation efficacy of the Li_2S/Co nanocomposite. Meanwhile, stable cyclability is achieved, indicating that such an additive does not have negative effect on the cathode materials (Figure 4c,d).

Furthermore, in addition to Li_2S/Co nanocomposite, other Li_2S/metal nanocomposite can also be synthesized for cathode prelithiation materials by employing other metal sulfides as the original reactants in the proposed chemical conversion technique. Herein, we also synthesized Li_2S/Fe nanocomposite through the chemical transformation reaction between lithium metal and natural occurring natural iron pyrite (FeS_2). Clearly, the starting FeS_2 is converted to mixed phases of Li_2S (JCPDS No. 23-0369) and Fe (JCPDS No. 06-0696) (**Figure 5**a and Figure S6, Supporting Information). Meanwhile, their small crystallite size is confirmed by the significant broadening of these XRD peaks. Some additional XRD peaks with low intensity can also be observed, which arise from the residue FeS_2 (JCPDS No. 42-1340) due to the uncompleted reaction between FeS_2 and lithium metal. The deep mixing of Li_2S and Fe with ultrafine particle size is verified by TEM and STEM images (Figure 5b,c). These structural features are similar to the Li_2S/Co nanocomposite, which are ideal for extracting lithium via the inverse conversion reaction ($Fe + 2Li_2S \rightarrow FeS_2 + 4Li^+ + 4e^-$) during the battery charge process. As expected, the first cycle charge capacity of the as-formed Li_2S/Fe nanocomposite is 495 mAh g^{-1} with the cutoff charge potential of 4.0 V versus Li^+/Li at the current density of 50 mA g^{-1}, while it delivers a negligible discharge capacity of 15 mAh g^{-1} with the cut-off discharge potential of 2.5 V (Figure 5d). Thus, a high "donor" lithium-ion capacity of 480 mAh g^{-1} is achieved in the first charge/discharge cycle, indicating high prelithiation efficiency. It is noteworthy here that the starting FeS_2 is an abundant and low cost natural product (pyrite). These, together with the high lithium-ion "donor" capacity, make the

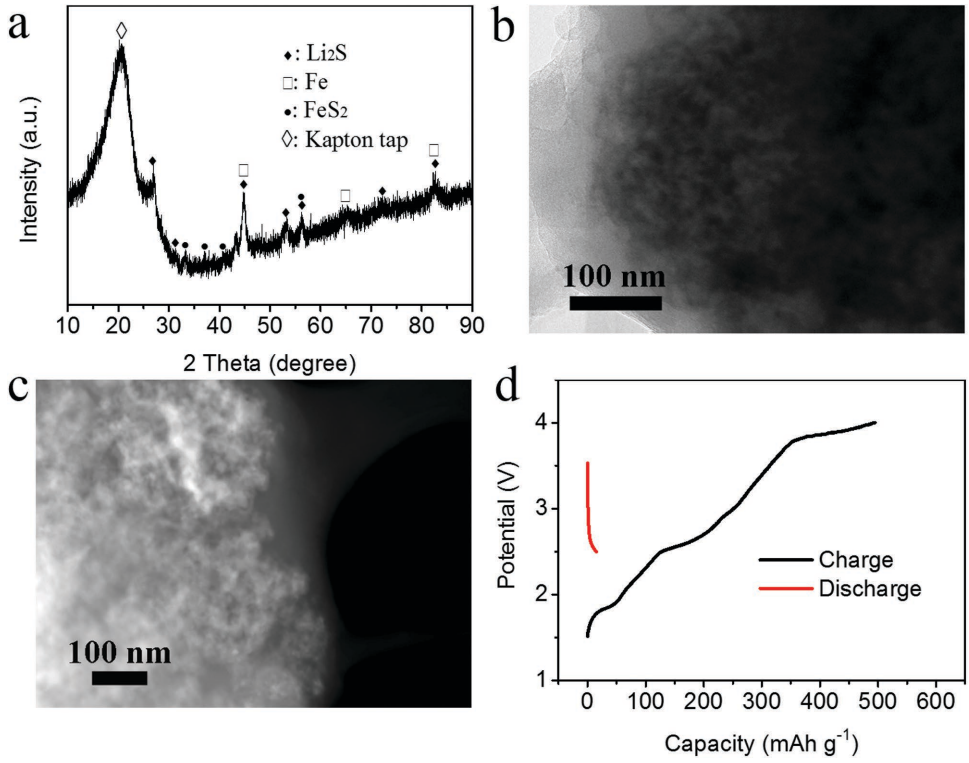

Figure 5. a) XRD pattern, b) TEM, and c) STEM images of the as-obtained Li_2S/Fe nanocomposite, and d) the initial charge and discharge curves of the pristine Li_2S/Fe electrode with the potential range of 4.0–2.5 V versus Li^+/Li at the current density of 50 mA g^{-1}. The XRD peak at 21° arises from the Kapton tape, which is used to protect Li_2S from moisture in the air.

Li_2S/Fe nanocomposite have promising industrial applications in current LIBs.

In conclusion, we have successfully synthesized a Li_2S/Co nanocomposite via a chemical conversion reaction between CoS_2 and molten lithium. The achieved Li_2S/Co nanocomposite has the characteristic of an electrochemical conversion reaction product with intimate mixing of polycrystalline Li_2S and metallic Co nanoparticles. When used as a cathode prelithiation material, the as-achieved Li_2S/Co composite undergoes an inverse conversion reaction instead of the decomposition of Li_2S upon charging. The Li_2S/Co nanocomposite exhibits a high OCV and affords a high "donor" lithium-ion specific capacity of 670 mAh g^{-1} in the cutoff potential range of existing cathodes. When incorporated into a $LiFePO_4$ cathode, the Li_2S/Co additive exhibits desirable lithium "donor" effect. Moreover, we have also demonstrated the successful chemical conversion of low-cost naturally occurring FeS_2 into a Li_2S/Fe nanocomposite with a high "donor" lithium-ion capacity. Due to the high "donor" lithium-ion capacities, potential compatibility with cathode materials, and battery fabrication processes, the as-synthesized Li_2S/metal nanocomposites can be used as promising cathode prelithiation materials for existing LIBs and for next-generation rechargeable lithium battery systems with larger initial lithium loss.

Supporting Information

Supporting Information is available from the Wiley Online Library or from the author.

Acknowledgements

Y.C. acknowledges the support from the Assistant Secretary for Energy Efficiency and Renewable Energy, Office of Vehicle Technologies of the U.S. Department of Energy under the Battery Materials Research (BMR) Program.

Received: January 24, 2016
Revised: March 13, 2016
Published online:

[1] M. Armand, J.-M. Tarascon, *Nature* **2008**, *451*, 652.
[2] J.-M. Tarascon, M. Armand, *Nature* **2001**, *414*, 359.
[3] C. K. Chan, H. L. Peng, G. Liu, K. McIlwrath, X. F. Zhang, R. A. Huggins, Y. Cui, *Nat. Nanotechnol.* **2008**, *3*, 31.
[4] X. L. Ji, K. T. Lee, L. F. Nazar, *Nat. Mater.* **2009**, *8*, 500.
[5] B. Scrosati, J. Hassoun, Y.-K. Sun, *Energy Environ. Sci.* **2011**, *4*, 3287.
[6] P. Verma, P. Maire, P. Novák, *Electrochim. Acta* **2010**, *55*, 6332.
[7] E. Peled, *J. Electrochem. Soc.* **1979**, *126*, 2047.
[8] K. Xu, *Chem. Rev.* **2014**, *114*, 11503.
[9] J. Hassoun, K.-S. Lee, Y.-K. Sun, B. Scrosati, *J. Am. Chem. Soc.* **2011**, *133*, 3139.
[10] N. Liu, L. B. Hu, M. T. McDowell, A. Jackson, Y. Cui, *ACS Nano* **2011**, *5*, 6487.
[11] D. Shanmukaraj, S. Grugeon, S. Laruelle, G. Douglade, J.-M. Tarascon, M. Armand, *Electrochem. Commun.* **2010**, *12*, 1344.
[12] C. R. Jarvis, M. J. Lain, M. V. Yakovleva, Y. Gao, *J. Power Sources* **2006**, *162*, 800.
[13] Z. H. Wang, Y. B. Fu, Z. C. Zhang, S. W. Yuan, K. Amine, V. Battaglia, G. Liu, *J. Power Sources* **2014**, *260*, 57.

[14] H. Zhao, Z. H. Wang, P. Lu, M. Jiang, F. F. Shi, X. Y. Song, Z. Y. Zheng, X. Zhou, Y. B. Fu, G. Abdelbast, X. C. Xiao, Z. Liu, V. S. Battaglia, K. Zaghib, G. Liu, *Nano Lett.* **2014**, *14*, 6704.
[15] M. W. Forney, M. J. Ganter, J. W. Staub, R. D. Ridgley, B. J. Landi, *Nano Lett.* **2013**, *13*, 4158.
[16] J. Zhao, Z. D. Lu, H. T. Wang, W. Liu, H.-W. Lee, K. Yan, D. Zhuo, D. C. Lin, N. Liu, Y. Cui, *J. Am. Chem. Soc.* **2015**, *137*, 8372.
[17] J. Zhao, Z. D. Lu, N. Liu, H.-W. Lee, M. T. McDowell, Y. Cui, *Nat. Commun.* **2014**, *5*, 5088.
[18] M. Noh, J. Cho, *J. Electrochem. Soc.* **2012**, *159*, A1329.
[19] M. G. Kim, J. Cho, *J. Mater. Chem.* **2008**, *18*, 5880.
[20] Y. M. Sun, H.-W. Lee, Z. W. Seh, N. Liu, J. Sun, Y. Z. Li, Y. Cui, *Nat. Energy* **2016**, *1*, 15008.
[21] Y. M. Sun, H.-W. Lee, G. Y. Zheng, Z. W. Seh, J. Sun, Y. B. Li, Y. Cui, *Nano Lett.* **2016**, *16*, 1497.
[22] Z. W. Seh, J. H. Yu, W. Y. Li, P.-C. Hsu, H. T. Wang, Y. M. Sun, H. B. Yao, Q. F. Zhang, Y. Cui, *Nat. Commun.* **2014**, *5*, 5017.
[23] Z. W. Seh, H. T. Wang, N. Liu, G. Y. Zheng, W. Y. Li, H. B. Yao, Y. Cui, *Chem. Sci.* **2014**, *5*, 1396.
[24] Z. W. Seh, H. T. Wang, P.-C. Hsu, Q. F. Zhang, W. Y. Li, G. Y. Zheng, H. B. Yao, Y. Cui, *Energy Environ. Sci.* **2014**, *7*, 672.
[25] F. X. Wu, H. Kim, A. Magasinski, J. T. Lee, H.-T. Lin, G. Yushin, *Adv. Energy Mater.* **2014**, *4*, 1400196.
[26] C. Nan, Z. Lin, H. Liao, M.-K. Song, Y. Li, E. J. Cairns, *J. Am. Chem. Soc.* **2014**, *136*, 4659.
[27] Z. W. Seh, W. Y. Li, J. J. Cha, G. Y. Zheng, Y. Yang, M. T. McDowell, P.-C. Hsu, Y. Cui, *Nat. Commun.* **2013**, *4*, 1331.
[28] Y. Yang, G. Y. Zheng, S. Misra, J. Nelson, M. F. Toney, Y. Cui, *J. Am. Chem. Soc.* **2012**, *134*, 15387.
[29] J. Gao, M. A. Lowe, Y. Kiya, H. D. Abruña, *J. Phys. Chem. C* **2011**, *115*, 25132.
[30] H. Hwang, H. Kim, J. Cho, *Nano Lett.* **2011**, *11*, 4826.
[31] S.-B. Son, T. A. Yersak, D. M. Piper, S. C. Kim, C. S. Kang, J. S. Cho, S.-S. Suh, Y.-U. Kim, K. H. Oh, S.-H. Lee, *Adv. Energy Mater.* **2014**, *4*, 1300961.
[32] R. B. Wu, D. P. Wang, X. H. Rui, B. Liu, K. Zhou, A. W. K. Law, Q. Y. Yan, J. Wei, Z. Chen, *Adv. Mater.* **2015**, *27*, 3038.
[33] Y. Kim, J. B. Goodenough, *J. Phys. Chem. C* **2008**, *112*, 15060.
[34] F. Zhou, S. Xin, H.-W. Liang, L.-T. Song, S.-H. Yu, *Angew. Chem. Int. Ed.* **2014**, *53*, 11552.
[35] Z. Yuan, H.-J. Peng, T.-Z. Hou, J.-Q. Huang, C.-M. Chen, D.-W. Wang, X.-B. Cheng, F. Wei, Q. Zhang, *Nano Lett.* **2016**, *16*, 519.
[36] P. Poizot, S. Laruelle, S. Grugeon, L. Dupont, J.-M. Tarascon, *Nature* **2000**, *407*, 496.
[37] H. Li, G. Richter, J. Maier, *Adv. Mater.* **2003**, *15*, 736.
[38] D. H. Son, S. M. Hughes, Y. D. Yin, A. P. Alivisatos, *Science* **2004**, *306*, 1009.
[39] M. T. McDowell, Z. D. Lu, K. J. Koski, J. H. Yu, G. Y. Zheng, Y. Cui, *Nano Lett.* **2015**, *15*, 1264.
[40] Q. M. Su, J. Xie, J. Zhang, Y. J. Zhong, G. H. Du, B. S. Xu, *ACS Appl. Mater. Interfaces* **2014**, *6*, 3016.
[41] I. Alstrup, I. Chorkendorff, R. Candia, B. S. Clausen, H. Topsøe, *J. Catal.* **1982**, *77*, 397.
[42] J. F. Moulder, J. Chastain, *Handbook of X-Ray Photoelectron Spectroscopy: A Reference Book of Standard Spectra for Identification and Interpretation of XPS Data*, Physical Electronics Division, Perkin-Elmer Corporation, Norwalk, CT, USA, **1995**.
[43] D. C. Higgins, F. M. Hassan, M. H. Seo, J. Y. Choi, M. A. Hoque, D. U. Lee, Z. Chen, *J. Mater. Chem. A* **2015**, *3*, 6340.
[44] L. Zhu, D. Susac, M. Teo, K. C. Wong, P. C. Wong, R. R. Parsons, D. Bizzotto, K. A. R. Mitchell, S. A. Campbell, *J. Catal.* **2008**, *258*, 235.
[45] Y. Ji, X. Y. Liu, W. Liu, Y. Wang, H. D. Zhang, M. Yang, X. F. Wang, X. D. Zhao, S. H. Feng, *RSC Adv.* **2014**, *4*, 50220.